



## Research Article

Theme: Lipid-Based Drug Delivery Strategies for Oral Drug Delivery  
Guest Editor: Sanyog Jain

# Erlotinib-Valproic Acid Liquisolid Formulation: Evaluating Oral Bioavailability and Cytotoxicity in Erlotinib-Resistant Non-small Cell Lung Cancer Cells

Ketan Patel,<sup>1,2</sup> Ravi Doddapaneni,<sup>1</sup> Manali Patki,<sup>2</sup> Vasanthkumar Sekar,<sup>1</sup> Arvind Bagde,<sup>1</sup> and Mandip Singh<sup>1,3</sup>

Received 13 October 2018; accepted 2 February 2019; published online 4 March 2019

**Abstract.** Lung cancer patients develop acquired resistance to tyrosine kinase inhibitors including erlotinib (ERL) after few months of primary treatment. Evidently, new chemotherapy strategies to delay or overcome the resistance are urgently needed to improve the clinical outcome in non-small cell lung cancer (NSCLC) patients. In this paper, we have investigated the cytotoxic interaction of ERL and valproic acid (VA) in ERL-resistant NSCLC cells and developed a liquisolid formulation of ERL-VA for improving oral bioavailability of ERL. ERL is weakly basic, biopharmaceutical classification system (BCS) class II drug with extremely poor aqueous solubility while VA is a branched chain fatty acid. Ionic interaction between ERL and VA (1:2 M ratio) resulted in significant enhancement in saturation solubility of ERL at different pH range. Liquisolid formulation of ERL-VA (EVLV) developed using PEG 400 and mesoporous calcium silicate was characterized for solid state and *in vitro* dissolution in biorelevant dissolution medium (FaSSIF and FeSSIF). Cytotoxicity of ERL was enhanced by 2–5 folds on co-incubation with VA in HCC827/ERL cell line. Flow cytometry analysis using AnnexinV-FITC assay demonstrated that VA and ERL alone have poor apoptotic effect on HCC827/ERL cells while combination showed around 69% apoptotic cells. Western blot analysis confirmed the role of survivin in overcoming resistance. *In vivo* pharmacokinetic studies of EVLV in rats demonstrated a 199% relative bioavailability compared to ERL suspension. Thus, EVLV could be a promising alternative to current ERL formulations in the treatment of NSCLC.

**KEY WORDS:** erlotinib; valproic acid; non-small cell lung cancer; drug resistance; liquisolid formulation.

## INTRODUCTION

Despite recent advances in understanding of the NSCLC biology and development of targeted chemotherapeutics agents, lung cancer has low survival rates. This is due to the emergence of resistance to tumor-targeted chemotherapeutics agents (1–3). Currently, surgery for operable tumors and chemotherapy with cisplatin, oxaliplatin, and gemcitabine are used for patients with advanced disease. Therapies targeted to tyrosine kinases (TKs) are small molecular inhibitors of epidermal growth factor

receptor-tyrosine kinase, *e.g.*, gefitinib (Iressa®) and erlotinib (Tarceva®). These are also used for the treatment of locally advanced or metastatic NSCLC that have failed at least one prior chemotherapy (2,4). Although tyrosine kinase inhibitors (TKIs) are the most widely used cancer targeted chemotherapeutics agents, toxicity and emergence of resistance have limited effectiveness and impact of TKIs. Statistics show that within 10–14 months of treatment, NSCLC patients start to develop resistance to erlotinib (ERL), which results in reoccurring of lung cancer (5,6). Thus, it is very imperative to develop new effective kinase inhibitors or agents to overcome resistance. Downregulation of the expression of the antiapoptotic protein survivin by EGFR-TKIs contributes to EGFR-TKI-induced apoptosis in EGFR mutation-positive NSCLC cells (7,8). Gatekeeper T790M mutation in EGFR promotes the development of resistance to EGFR TKIs. The second-generation TKIs such as dacomitinib and afatinib inhibit EGFR T790M mutant but these TKIs have failed to demonstrate compelling responses in clinical trials (9).

Restoring the chemosensitivity of TKIs using FDA-approved molecules could be a simple and fast-track approach compared to the development of new TKIs for the

Guest Editor: Sanyog Jain

**Electronic supplementary material** The online version of this article (<https://doi.org/10.1208/s12249-019-1332-0>) contains supplementary material, which is available to authorized users.

<sup>1</sup> College of Pharmacy and Pharmaceutical Sciences, Florida A&M University, Tallahassee, Florida 32307, USA.

<sup>2</sup> College of Pharmacy and Health Sciences, St. John's University, Queens, New York 11439, USA.

<sup>3</sup> To whom correspondence should be addressed. (e-mail: mandip.sachdeva@fam.u.edu)

treatment of ERL-resistant lung cancer. Survivin is overexpressed in most of the tumors and is reported to play a significant role in development of chemotherapeutic resistance, increased tumor recurrence, and shorter patient survival. Okamoto *et al.* 2011 have demonstrated that activation of the AKT-survivin pathway induced by PTEN loss underlies a mechanism of resistance to erlotinib-induced apoptosis in EGFR mutation-positive NSCLC (8). They also indicated that targeting survivin could potentially be helpful in overcoming EGFR-TKI resistance in EGFR mutation-positive NSCLC. Epigenetic modulators, especially histone deacetylase (HDAC) inhibitors, act as antiproliferative agents by downregulating survivin in various cancer cells. Valproic acid (VA), an antiepileptic molecule, is one the most widely explored HDAC inhibitor in various *in vitro* and *in vivo* anticancer studies, alone and in combination with chemotherapeutic agents. VA favors hyperacetylation of histone N-terminal tails, restores a negative charge, and decreases their affinity for DNA, leading to decondensation and transcriptional activation (7,10,11).

ERL has extremely poor aqueous solubility with low oral bioavailability. It has a large intra- and inter-patient variability in peak plasma concentration and area under the curve (AUC) (12,13). ERL is available as a hydrochloride salt (Tarceva®) which is also sparingly soluble in aqueous phase especially at intestinal pH. Therefore, there is a need of a formulation to enhance solubility and bioavailability of ERL. VA (2-propylpentanoic acid) is a short-branched chain fatty acid with an oil like characteristic. Our goal was to co-formulate ERL and VA using a biocompatible solubilizer, *e.g.*, PEG 400. However, long-term stability of liquid formulation filled capsule is a big concern. Transforming liquid lipid formulations into liquisolid form has been one of the topmost industrial interests. Liquisolid technique is a simple, economical, and commercially viable option to improve the solubility of BCS class II and IV drugs (14,15). Drug solubilized in biocompatible organic solvent with or without surfactant. They are also solubilized in a self nano/microemulsifying preconcentrate and then adsorbed onto an inert and microporous inorganic pharmaceutical excipient, *e.g.*, Neusilin US2, Aerosil 200, and Syloid 244 FP *etc.*

The aims of our research work were to (i) to investigate the chemosensitizing effect of VA on TKIs resistant NSCLC cells and (ii) to enhance aqueous solubility, dissolution, and bioavailability of ERL by formulating a ERL-VA liquisolid formulation (EVLf).

## MATERIAL AND METHODS

Erlotinib (99%) was purchased from AK Scientific Inc. (Union City, CA). Florite PS 200 and Neusilin US2 were received as gift samples from Tomita Pharmaceutical Co. Ltd., Japan, and Fuji Chemicals, Japan, respectively. Aerosil 200 and Aerosil 972 were purchased from Evonik Corporation (Parsippany NJ, USA). Annexin V-fluorescein isothiocyanate (FITC) Apoptosis Detection Kit was purchased from BD Bioscience, CA, USA. PEG 400 was received as a gift sample from BASF (Tarrytown NY, USA). DMEM, EMEM medium, fetal bovine serum, and other cell culture materials were purchased from Lonza (Basel, Switzerland). Coumarin-6, HPLC grade solvents, and salts were procured from Sigma-Aldrich Co (ST. Louis, MO, USA).

## Cell Culture

HCC827 cell lines were obtained from American Type Culture Collection. ERL-resistant HCC827 was developed by continuous exposure of low dose ERL for 3 months (16). All the cell lines were cultured in DMEM medium supplemented with 10% FBS, 2 mM glutamine, 100 units per ml penicillin, and 100 mg/ml streptomycin.

## Animal Studies

The pharmacokinetic behavior of ERL and EVLF was performed in SD rats (160–220 g). The study protocol was approved by the Institutional Animal Care and Use Committee, Florida A & M University. Rats were acclimatized and given standard animal diet, in a controlled room (22 ± 1°C at 35–50% RH) for a week prior to experiments. The animals were divided according to body weight into two groups, ERL suspension and EVLF and each group having six animals.

## HPLC Method and Extraction of ERL from Plasma Samples

An HPLC method was developed and validated for ERL quantification using HPLC system (Waters WAT053502) consisting of a pump (WAT054275) with integrated system controller auto sampler (e2695 separations module) and variable wavelength UV detector diode array detector (2996, Waters). Data acquisition and analysis was performed in post-run analysis using Empower software (Waters Corporation). The column and HPLC system was kept in ambient condition throughout the development and validation procedure. We employed C18 Luna® (Phenomenex®, 250 × 4.6 mm) column with 5 µm sphere shape particles, 100 Å pore size, 400 m<sup>2</sup> g surface area 13.5% carbon load, and calculated bonded phase coverage of 5.50 µmole/m<sup>2</sup>. The spectrum analysis was carried out between 200 and 400 nm and the fixed wavelength measurement was recorded at 246.00 nm. A mixture of 10 mM ammonium acetate buffer (pH 4.2) and acetonitrile (40:60, v/v) as the mobile phase was optimized and maintained at 1 ml/min flow rate. The typical best fit linear regression equations of the developed HPLC method was peak area (mV s) = 586.5 × conc. (ng/mL) + 4176 with r<sup>2</sup> = 0.996 in the concentration range of 30–1200 ng/mL of erlotinib in plasma. The system suitability parameters k, T, HETP, Neff, HEFF, and h showed that the developed 3D view method has good reproducibility. The LOD and LOQ of the developed HPLC method were 25 and 30 ng/ mL respectively. The accuracy study result of the developed HPLC method demonstrated that the %R.S.D. was less than 2.34 with mean % recovery range from 97.27 to 104.34. The intra-day precision (%R.S.D.) study results of the developed HPLC method was in the range of 0.23 to 1.84 respectively. The repeatability of the precision samples on three different occasions within a day was always less than 1.10 with least %R.S.D. of 0.13 respectively. The plasma concentration of ERL vs. time was plotted for pure drug suspension and EVLF formulations. The plasma samples were processed for extraction of ERL by protein precipitation method. The plasma samples (100 µL) were mixed with acetonitrile and methanol (1:1, 300 µL), vortexed for 10 min, and then centrifuged at 12,000 rpm for 10 min. The

supernatant layers were injected into the HPLC system with injection volume hundred microliters. ERL in plasma was estimated by developed and validated HPLC diode array method.

### Optimization of ERL:VA Molar Ratio

Initially, various batches were prepared by solubilizing ERL in various ratio of VA and PEG (PEG 400) (Table I). The mixtures were vortexed for 10 min to facilitate solubilization. To evaluate the saturation solubility in water, 100  $\mu$ l of each formulation was added to 5 ml of water and kept on a shaker at 37°C for 24 h. Samples were centrifuged at 10,000 rpm for 10 min. The supernatant was suitably diluted with mobile phase and the ERL concentration was quantified using HPLC. Comparative evaluation of saturation solubility of ERL-PEG 400 (free base), ERL HCl (salt), and ERL-VA-PEG 400 (optimized batch) was carried out in pH 1.2 and pH 6.8. Each of the above components was weighed accurately and was diluted with aqueous medium—pH 1.2 and pH 6.8, respectively. The samples were vortexed using a cyclomixer for 5 min to facilitate dispersion of samples in aqueous phase and were kept on shaker for 24 h at 37°C. After 24 h, precipitated ERL was separated using centrifugation (10,000 rpm, 5 min). Fifty microliters of clear supernatant was collected and mixed with HPLC mobile phase for assessing the concentration of ERL in supernatant.

### Particle Size Analysis

The particle size and polydispersity index of different formulations prepared were determined using DLS particle size analyzer (Malvern Zetasizer Nano ZS, UK). Batches were diluted with HPLC grade water to ascertain that the light scattering intensity was within the optimum range of the instruments' sensitivity. The diluted samples were placed into the cuvette and the data was analyzed. All experiments were carried out in triplicates.

### Formulation Development

ERL was solubilized in PEG 400 with the addition of VA in 1:2 M ratio. ERL-VA Liquid Formulation (EVLV) was prepared by drop-wise addition of ERL-VA-PEG 400 solution on an inert solid carrier like inorganic microporous silica (Neusilin US2, Florite PS 200, Aerosil 972 Aerosil 200) in glass mortar. Type and amount of adsorbent required to convert liquid formulation into free-flowing powder was optimized. For microscopic analysis, 0.5 mg of fluorescent dye—coumarin-6—was dissolved in ERL-VA-PEG 400 and mixed with 1 g of various adsorbent in mortar pestle. Drug solution was added in increments of 100  $\mu$ L till adsorbent blend became sticky.

### Solid State Characterization

#### Differential Scanning Calorimetric (DSC) Analysis

The DSC analysis was carried out using the DSCQ100 System (TA Instrument, USA) to ascertain the physical state of ERL in EVLV. Briefly, 5 mg of the ERL, blank

formulation, Florite PS 200, and EVLV were weighed individually and sealed hermetically into an aluminum pan. The samples were heated at a temperature range of 35 to 250°C with a heating rate of 5°C/min under nitrogen purge. All data were analyzed using the Universal Software analysis 2000 (TA Instrument, USA).

#### Powder XRD Studies

X-ray powder scattering measurements of ERL, physical mixture, and EVLV were recorded using a Shimadzu XRD-6000 diffractometer (Shimadzu, Kyoto, Japan). It is equipped with Ni filter. Monochromatic Cu-K $\alpha$  radiation source was used to record PXRD diffraction patterns for the determination of the presence of crystals in EVLV. The scanning range (2 $\theta$ ) used was from 0° to 60° at the rate of 2°/min.

#### In vitro Dissolution Study

*In vitro* dissolution analysis was carried out using USP apparatus II at 37  $\pm$  0.5°C, at 75 rpm, in 500 ml of 0.1 N HCl and biorelevant media [Fasted State Simulated Intestinal Fluid (FaSSIF) and Fed State Simulated Intestinal Fluid (FeSSIF)]. Biorelevant media was prepared using the procedure described previously (17). ERL and EVLV equivalent to 50 mg ERL were added and aliquots were withdrawn at 10, 20, 30, 45, and 60 min with simultaneously replacing the same volume with fresh medium each time. The aliquots were centrifuged at 10,000 rpm for 10 min and supernatant was mixed with HPLC mobile phase before HPLC analysis.

#### In vivo Pharmacokinetic Study

The rats were fasted overnight before ERL and EVLV administration and had access to water and *ad libitum*. Animals were given 100 mg/kg equivalent dose of ERL suspension and EVLV by oral route. For each time point, 300  $\mu$ L of blood samples was collected from tail vein and the samples were immediately transferred into Microvette® 500 Z-gel tubes. The blood samples were centrifuged at 5000 rpm for 10 min at 4°C to obtain plasma samples. The sample collection time points were 10, 30, 60, 120, 240, 360, 480, 600, 720, 1080, and 1440 min after drug administration. All the samples were stored at -20°C until analysis and thawed before HPLC analysis. All the pharmacokinetic parameters were calculated by non-compartment model using WinNonlin software (Version 2.1, Pharsight Corporation and USA).

#### In vitro Cytotoxicity Study

ERL-resistant HCC827 cells were seeded in a 96-wells (1  $\times$  10<sup>3</sup> per well) and incubated overnight. The cells were treated with various concentrations of ERL, ERL + VA (0.5 mM), and VA (0.5 mM) alone. After 48 h, the cells were washed with Dulbecco's phosphate-buffered saline (DPBS) and fixed in 100  $\mu$ l glutaraldehyde solution (0.25% v/v in water) and incubated at 37°C for 30 min. Glutaraldehyde was aspirated and 100  $\mu$ l crystal violet solution (0.4% w/v) was added and incubated at room temperature for 15 min. Crystal violet solution was aspirated, plates were washed with DPBS, and SLS (0.5% w/v) solution was added to dissolve

**Table I.** Composition and Drug Loading of Various Batches

Batches	Composition			
	ERL (mg)	PEG 400 ( $\mu$ L)	VA ( $\mu$ L)	%Drug loading
B0	50	500	0	10
B124	50	480	20	10
B226	50	640	20	7.5
B329	50	980	20	5
B444	50	460	40	10
B546	50	620	40	7.5
B649	50	960	40	5
B784	50	420	80	10
B885	50	580	80	7.5
B989	50	920	80	5

the crystal violet. The absorbance of crystal violet was read at 540 nm and percentage cell kill data was acquired to calculate IC50.

#### Apoptosis Assay

Flow cytometric analysis of untreated and treated HCC 827/ERL cells was carried out using an Annexin V-FITC Detection Kit and BD FACSCalibur according to the manufacturer's instructions. HCC 827/ERL cells were seeded into 6 well plates and after overnight incubation treated with ERL, VA (0.5 mM), and ERL + VA (0.5 mM). After 48 h, cells were resuspended in the binding buffer, mixed with Annexin V-FITC reagent, and incubated for 30 min at room temperature in the dark. Samples were analyzed by BD FACSCalibur (BD Biosciences) using the standard optics for detecting FL1 (FITC) and FL2 (PI). Data were analyzed using CellQuest WinMDI software (BD Bioscience, San Jose, CA, USA).

#### Immunoblot

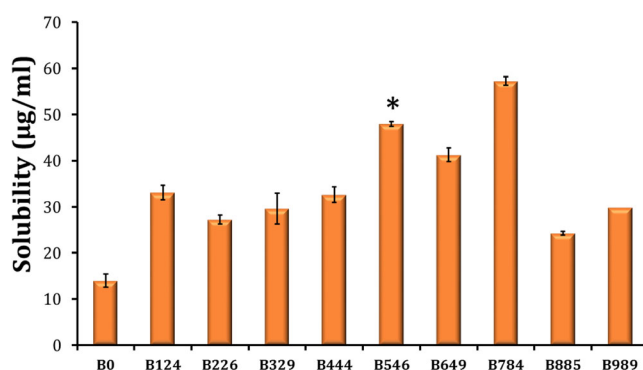
To examine the effects of VA on protein levels in the cultured cells, HCC 827/ERL cells were treated with PBS (control), ERL, VA, or ERL + VA for 48 h. Next, the cells were lysed in 300  $\mu$ l of homogenization buffer (1) and centrifuged for 15 min at 14,000 rpm at 4°C. The resulting supernatant was collected and protein concentration was determined by bicinchoninic acid assay (Pierce Biotechnology, IL, USA). Protein (30–50  $\mu$ g) was fractionated by SDS-PAGE and transferred onto nitrocellulose membrane (Bio-Rad) by electroblotting. The membrane was blocked with 3% w/v BSA in PBS-Tween 20 (PBST) for 3 h at room temperature. The membrane was incubated with primary antibodies (survivin, caspase 3,  $\beta$ -actin) overnight at 4°C with 3% w/v BSA in PBST according to the antibody data sheets. After washing with PBST for 15 min, the membrane was incubated with the appropriate secondary antibodies, and proteins were detected by the enhanced chemiluminescence system (Bio-Rad).

## RESULTS

### Optimization of ER:VA Ratio

Table I depicts the composition of various formulation batches prepared for optimization of ERL:VA:PEG 400 ratio and drug loading to achieve maximum aqueous solubility of ERL. Batches with 20  $\mu$ L, 40  $\mu$ L, and 80  $\mu$ L VA represent ERL:VA molar ratio of 1:1, 1:2, and 1:4, respectively. Results of saturation solubility of various ERL formulations are given in Fig. 1. The solubility of all the batches prepared using VA showed significantly higher saturation solubility ( $p < 0.01$ ) than ERL/PEG 400 (14  $\mu$ g/ml) and pure ERL (0.7  $\mu$ g/ml). The lowest solubility of VA free batch (B0) compared to batches composed of VA (B124 to B989) clearly justified the role of VA in enhancing aqueous solubility of ERL. At 1:1 M ratio (ERL:VA), the solubility was found to be between 27 and 33  $\mu$ g/ml irrespective of the concentration of the PEG 400 while a substantial increment in aqueous solubility was observed at 1:2 M ratio ( 50  $\mu$ g/ml).

Surprisingly, at 1:4 M ratio, concentration of PEG 400 affected the solubility of ERL. Despite the lowest amount of PEG 400 in B784 (highest drug loading), it showed the highest solubility of ERL (57.26  $\mu$ g/ml). Increasing the concentration of PEG 400 led to a drastic reduction in solubility to 29.92  $\mu$ g/ml. There was no substantial increment in solubility of ERL with increase in the molar ratio of ERL:VA from 1:2 to 1:4. Even though, highest solubility was achieved at 1:4 M ratio (ER:VA), B546 with 1:2 M ratio of

**Fig. 1.** Saturation solubility of various ERL batches

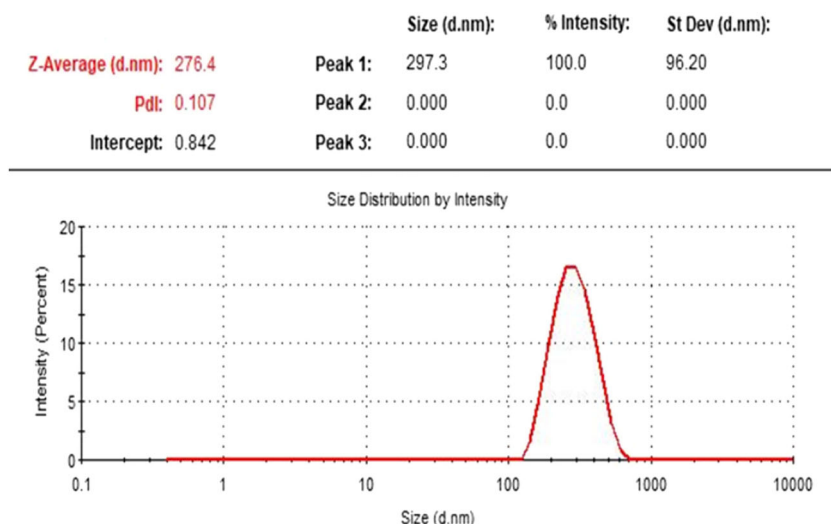


**Fig. 2.** Dynamic light scattering particle size analysis of B546

ERL:VA and 7.5% *w/v* drug loading was optimized. This was selected for further studies due to following reasons; B784 led to the formation of very large particles (particle size of > 1  $\mu\text{m}$ ) due to extensive agglomeration resulting in a formation of an unstable system, whereas B546 and B649 formed a self-assembled nanosystem on dispersion with water. Interestingly, B546 formed a self-assembled structure of 276.4 nm with unimodal distribution (polydispersity index, 0.107) (Fig. 2). Similarly, Batch B649 showed a particle size of 380.4 nm with polydispersity index of 0.1. Such a formation of a self-assembled nanosystem was not observed with any other batches which clearly suggested that ratio of ERL:VA:PEG 400 is very crucial in formation of a self-assembled nanosystem.

As shown in Fig. 3, the aqueous solubility of ERL is dependent on pH and type of formulation. It is obvious that solubility of ERL should be higher at lower pH due to the basic nature of the drug. Interestingly, solubility of ERL-VA-PEG 400 formulation was nearly doubled compared to its hydrochloride salt at pH 1.2. Similarly, solubility of ERL-VA-PEG 400 was found to be 2.7 times higher than its hydrochloride salt at pH 6.8.

### Liquisolid Formulation Development

Among the various adsorbents (Florite PS 200, Aerosil 972, Aerosil 200, and Neusilin US2) screened for the adsorption of ERL/VA/PEG400 solution, Florite PS 200 (calcium silicate) was found to be the most suitable for the preparation of liquisolid formulation. Free-flowing powder was obtained at 2.5:1 weight ratio of drug solution:Florite PS 200. Whereas, other adsorbents gave sticky and poorly flowable granules even at a lowest weight ratio of 1:1 drug solution:adsorbent (Fig. 4(A)). Therefore, Florite PS 200 was selected as an adsorbent for further studies. Optimized ERL-VA liquisolid formulation (EVLF) was composed of 50 mg ERL, 40  $\mu\text{L}$  VA, 620  $\mu\text{L}$  PEG 400, and 250 mg Florite PS 200. Microscopic evaluation of coumarin 6 loaded EVLF is shown in Fig. 4(B). Fluorescence microscopic image of Florite PS 200 particle clearly demonstrated the deeper and uniform penetration of ERL solution in porous structure of Florite PS 200.

### Solid State Characterization

As shown in Fig. 5(A), DSC thermogram of pure ERL showed a sharp endothermic peak due to the melting of crystalline API. No such peak was observed in case of Florite 200, blank formulation, and EVLF. It means that the drug did not crystallize upon adsorption and remained in a solubilized state within EVLF. Powder X-ray diffraction (PXRD) patterns are shown in Fig. 5(b). ERL characteristics peaks were observed at the diffraction angles (11.2°, 14.6°, 16.3°, 22.4°, 23.4°, 20.1°, 24.6°, 27.6°) showing a typical crystalline pattern. Florite 200 displayed no crystalline peak due to its amorphous nature. The major characteristic peaks for the drug were observed in the physical mixtures, especially at 24.6° and 27.6°. These results are similar to the previous reports (12,13). Importantly, characteristic peaks of ERL were not observed in EVLF. Therefore, consistent with the DSC data, this result further confirmed that ERL did not precipitate out and remained in the solubilized state in the EVLF.

### In vitro Dissolution Study

EVLF showed rapid and complete dissolution of ERL within 5 min while ERL API showed less than 25% ERL

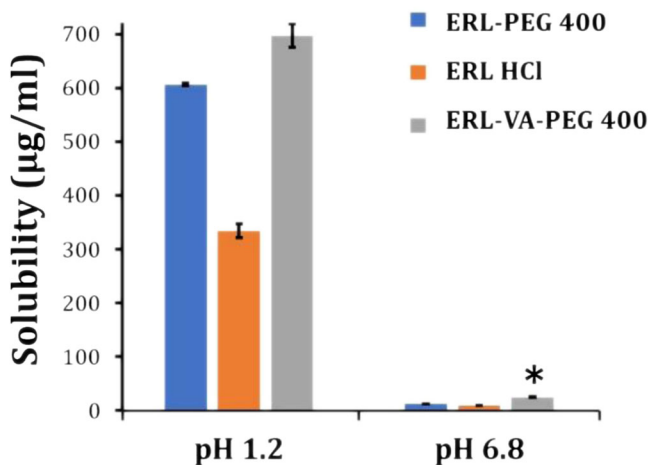


**Fig. 3.** Saturation solubility at different pH

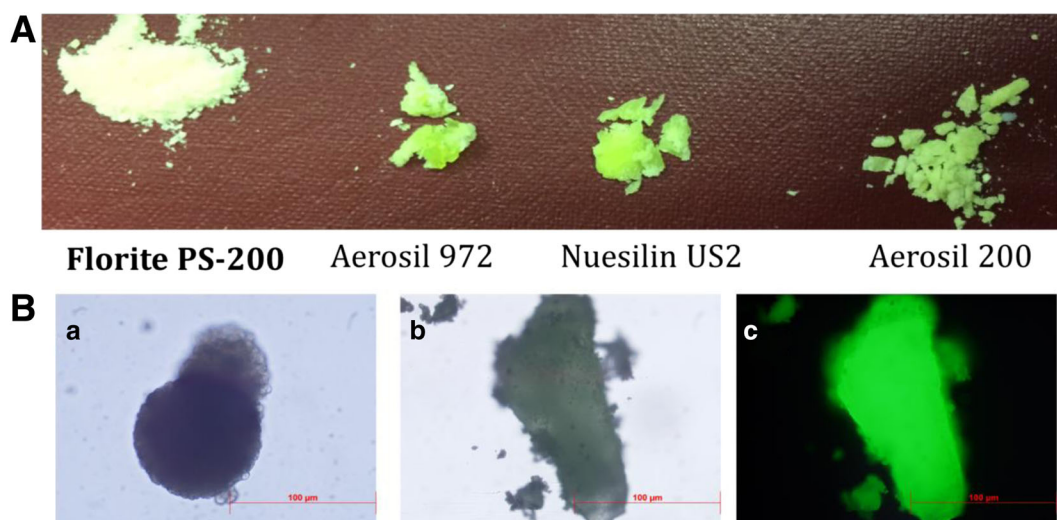


**Fig. 4.** Screening of adsorbents for liquid formulation of ERL-VA. **A** Adsorption of ERL/VA/PEG 400 on various inorganic adsorbents. **B** Microscopic images ( $\times 10$ ) of **a** Florite PS 200 **b** bright field image of EVLF, and **c** fluorescence image of EVLF loaded with coumarin-6

release up to 60 min in 0.1 N HCl (Fig. 6(a)). Percentage of ERL dissolved from EVLF is  $\sim 4$ – $5$  times higher than the plain drug in non-sink conditions. Further, in EVLF at 60 min, there was no reduction in the %ERL dissolved which indicated that ERL did not precipitate out in a dissolution media, confirming its complete solubilization. Figure 6(B) shows the dissolution of ERL in biorelevant media (FaSSIF and FeSSIF). In FaSSIF and FeSSIF within 5 min, the % drug dissolved (ERL API) was found to be 1.1% and 13% respectively. EVLF showed nearly 9 and 3 fold higher dissolution than API in FaSSIF and FeSSIF, respectively.

#### *In vivo* Pharmacokinetic Study

The *in vitro* dissolution profile of EVLF showed that the drug is released immediately and almost 100% ERL is released within 5 min (Fig. 6(a)). This *in vitro* release of drug by EVLF formulation is reflected in the *in vivo* pharmacokinetic study with  $T_{max}$  of  $120.00 \pm 5.25$  min with high  $t_{1/2}$  (Table II). There was more than a twofold increase in  $AUC_{0-\infty}$  of the prepared EVLF formulation compared to

ERL suspension. These results indicated that EVLF had a much higher rate and extent of bioavailability compared to ERL suspension. The  $C_{max}$  values of EVLF formulation were  $380.11 \pm 22.14$  ng/mL which is significantly greater than that of the reference suspension formulation ( $284.21 \pm 11.87$  ng/mL,  $p < 0.05$ ). The non-compartment analysis showed that the MRT of ERL suspension was much lower when compared to the EVLF formulation ( $634.70 \pm 12.44$ ). These pharmacokinetic parameters demonstrate that ERL loaded EVLF maintains the plasma concentration of ERL for a longer time than the suspension formulation. Hence, the ERL-loaded EVLF showed very low clearances rate of  $0.00034$  (mg)/(ng/mL)/min when compared to ERL suspension (Fig. 7).

#### *In vitro* Cytotoxicity Study

Cytotoxicity of ERL was significantly enhanced by co-incubation with VA in ERL-resistant HCC827 cells. As shown in Fig. 8, ERL showed  $< 15\%$  cell killing even at the highest concentration of  $25 \mu\text{M}$  in HCC827/ERL cells. VA also did not show significant cell killing at  $0.5$  mM.

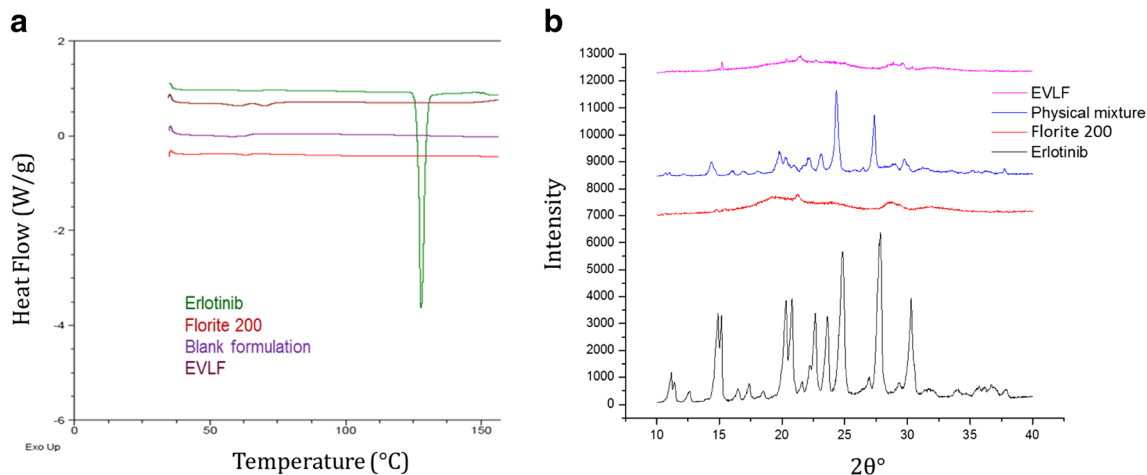


**Fig. 5.** Solid state characterization **a** DSC thermograms **b** Powder X-ray diffraction (PXRD)

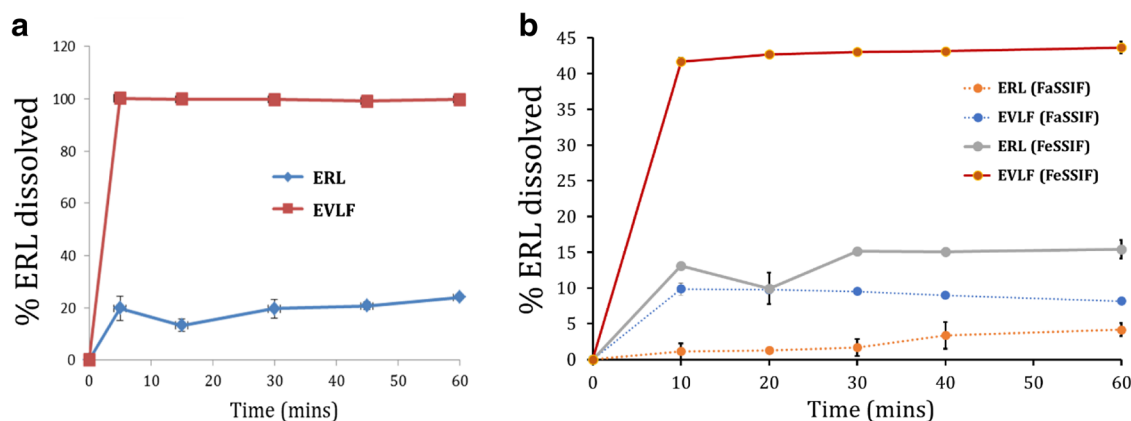


**Fig. 6.** **a** Dissolution profile of ERL and EVLF in 0.1 N HCl. Percentage of ERL dissolved from EVLF is ~4–5 times higher than plain drug. **b** Dissolution profile of ERL and EVLF in FaSSIF and FeSSIF. EVLF showed nearly 9 and 3 fold higher dissolution than API in FaSSIF and FeSSIF, respectively

Importantly, ERL showed higher cytotoxicity when co-incubated with a non-cytotoxic concentration of VA. Cytotoxicity of ERL was enhanced by 4.6-fold and 3.5-fold at 25  $\mu$ M and 12.5  $\mu$ M concentration, respectively. However, no enhancement in the cytotoxicity of ERL was observed at lower concentrations.

#### Apoptosis Assay

Results of Annexin V-FITC apoptosis analysis were in complete agreement with the cytotoxicity studies. Cells treated with combination of ERL-VA showed a significantly high number of apoptotic cells (69.9%) compared to the ERL treated cells (14.4%), as assessed by flow cytometry analysis (Fig. 9). Control, VA, and ERL-treated groups showed a significantly higher number of viable cells compared to ERL + VA treated group.

#### Western Blot Analysis

To explore the status of survival and apoptotic protein expression, we further tested these proteins by western blot analysis. We induced ERL-resistant lung cell carcinoma cell line (HCC 827-4  $\mu$ M ER). As shown in Fig. 10, combination of VA and ERL led to a significantly ( $p < 0.01$ ) downregulated the expression of survivin (1.1-fold) in HCC 827-4  $\mu$ M

ERL compared to the control. Accordingly, upregulated the expression of caspase-3 (0.6-fold) was significantly ( $p < 0.05$ ) observed in combination compared to the only ERL treatment, indicating that VA might reverse TKI resistance of cancer cells that in turn initiate mitochondrial apoptotic pathway. Therefore, we hypothesized that targeting survivin in TKI-resistance lung cancer cells could reverse the resistant phenotype in tumor cells, thereby enhancing the therapeutic efficacy of ERL. Interestingly, the results showed that the treatment with a combination of VA and ERL significantly led to a decrease in cell survival. It also led to an increase in cell apoptosis for TKI-resistant HCC827-ERL cells, relative to those treated with VA or ERL alone.

#### DISCUSSION

Research work was aimed to address the following key problems associated with erlotinib-based therapy: (1) Development of resistant within few months of treatment, and (2) poor aqueous solubility and oral bioavailability. We hypothesized that use of ERL and VA in combination could potentially solve both the issues. VA (2-propyl-pentanoic acid) is an 8-carbon branched chain fatty acid. Being a short chain fatty acid, oil like characteristic of VA could be helpful in solubilization of lipophilic drug. At the same time, favorable interaction between carboxylic group of VA and

**Table II.** Non-compartment Pharmacokinetic Parameters of ERL suspension and EVLF

Parameter	Unit	ERL suspension	ERL SNEEDS	
1	AUC <sub>0-t</sub>	ng/ml*min	133,210.90 $\pm$ 95.21	266,253.04 $\pm$ 288.22
2	AUC <sub>0-inf</sub>	ng/ml*min	139,022.54 $\pm$ 189.98	295,600.31 $\pm$ 542.14
3	AUMC <sub>0-inf</sub>	ng/ml*min <sup>2</sup>	44,450,032.80 $\pm$ 785.95	187,610,766.60 $\pm$ 1254.25
4	MRT <sub>0-inf</sub>	min	320.74 $\pm$ 18.21	634.70 $\pm$ 12.44
5	t <sub>1/2</sub>	min	115.10 $\pm$ 8.32	404.90 $\pm$ 24.58
6	T <sub>max</sub>	min	240 $\pm$ 2.54	120.00 $\pm$ 5.25
7	C <sub>max</sub>	ng/ml	284.21 $\pm$ 11.87	380.11 $\pm$ 22.14
8	Vz/F	(mg)/(ng/ml)	0.12 $\pm$ 0.03	0.20 $\pm$ 0.02
9	Cl/F	(mg)/(ng/ml)/min	0.00072 $\pm$ 0.0004	0.00034 $\pm$ 0.00001
10	k <sub>el</sub>	(min <sup>-1</sup> )	0.006	0.002
11	RB	%		199.90

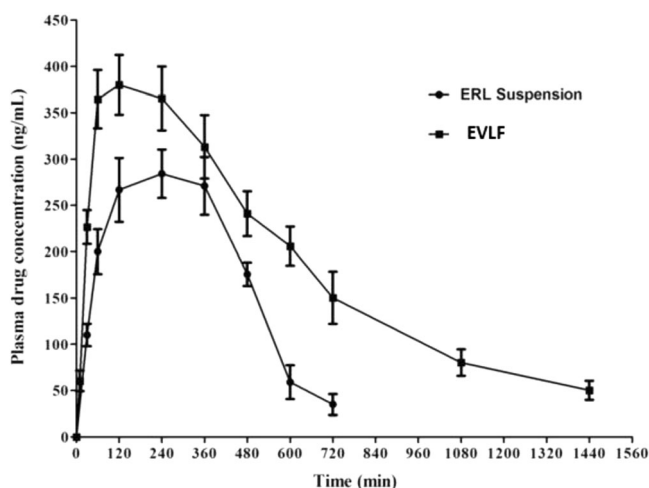


**Fig. 7.** Plasma drug concentration vs. time profile of ERL and EVLF in rats

amine group of ERL could result in enhanced aqueous solubility of ERL. Another potential benefit of this combination is overcoming the ERL resistant in lung cancer due to HDAC inhibition mediated reduction in surviving level. Thus, in this paper, biopharmaceutical and pharmacological benefits of ERL and VA combination were investigated.

Development of chemoresistance to TKIs over few months of treatment is one of the major challenges in NSCLC (1,5,6). Various approaches have been reported but their outcomes are limited to clinical studies. One of key mechanism of development of TKIs resistant was an elevation of survivin in NSCLC cells after prolong treatment with TKIs, considering this fact, we used a survivin inhibitor to overcome the resistance of ERL in ERL-resistant NSCLC cells (7,8). Survivin is a unique member of the inhibitor of apoptosis protein (IAP) family that acts as a suppressor of apoptosis and plays a central role in cell division. Survivin is massive upregulated in various human tumors and involved in tumor progression and development of resistance (7,18,19). In the current study, treatment with HDAC-inhibitor VA decreased survivin expression significantly in treatment of VA + ERL combination. Our observation was in complete agreement with the previous preclinical studies which demonstrated that downregulation of survivin expression leads to increase the apoptotic and sensitized tumor cells to chemotherapeutic drugs and radiation in different human tumor models. Previous report showed that HDAC inhibitor VA can induce apoptosis and re-expression of epigenetically silenced tumor suppressor genes in cancer cells. The HDAC inhibitor, VPA, counteracted erlotinib resistance in lung cancer cells, evidenced by a significant increase in caspase 3 indicated that it induces TKI-resistant lung cancer cells to apoptotic pathway. Consequently, combination of both HDAC inhibitor VA and ERL may delay or prevent TKI-drug resistance of lung cancer. A study by Zhang *et al.* 2012 reported that knock-down of HDAC2 completely mimicked the effects of VPA on survivin and cell migration, and over-expression of survivin could also rescue the effects of HDAC2 knockdown on cell migration (11). Figure 11 shows schematic representation of role and proposed mechanism of VA in enhancing solubility and overcoming resistant in ERL-resistant lung cancer.

The observed increase in solubility could be due to ionic interaction (acid-base) of the drug with VA which has structural similarity to short chain fatty acid. Lipophilic chain of VA might help in solubilizing lipophilic part of ERL while terminal acid group interact with amine of ERL to improve its solubility. Ionic interaction of ERL and VA was further confirmed by zeta potential study. The blank valproic acid formulation (no ERL) showed a zeta potential of  $-0.359$  mv whereas the B546 batch (ERL + VA + PEG400) has zeta potential of  $+42.9$  mv. The blank formulation has a neutral to negative charge due to absence of any ionizable group on the surface of nanoglobule, whereas the positive zeta potential of the B546 batch confirmed the presence of ionized ERL on the surface. Zeta potential graphs of both the formulation are given as the [supplementary file](#). Polydispersity index close to 0.1 confirmed the formation of self-assembled nanosystem due to favorable interaction between ERL, VA, and PEG 400. Poor bioavailability of ERL is attributed by its extremely poor water solubility. There are scanty of report demonstrating enhancement in solubility of ERL which includes solid dispersion and self-emulsifying formulation (12,13,20,21). Since our *in vitro* cell culture data emphasized on use of VA in combination with ERL for overcoming the resistance, we investigated VA as a solubility enhancing agent for ERL. ERL is a weakly basic hydrophobic molecule while VA is a short-branched chain fatty acid. As expected, due to ionic interaction between ERL and VA, solubility of ERL was significantly enhanced (Fig. 11). Ionic complexation between ERL and VA, lipophilicity of VA, and co-solvency effect of PEG 400 are collectively responsible for the enhanced aqueous solubility of ERL. We hypothesized that ERL is present in the solubilize form within VA nanodroplets stabilized by PEG 400. Enhancement in the solubility of weakly basic drug by fatty acid (*e.g.*, lumefantrine and oleic acid) has been reported previously (22). Liquid formulation has several limitations, and therefore, it is quintessential to convert such liquid formulation into solid formulation to enhance the physicochemical stability, handling, and commercial feasibility (14,23). Porous structure of Florite PS 200 provided enormous surface area for rapid interaction of dissolution media with ERL-VA-PEG 400 solution. Florite PS 200 is a synthetic mesoporous calcium silicate with exceptional liquid absorption capacity due to deep and large micropore within it. Neusilin US2 is microporous granular particles of magnesium

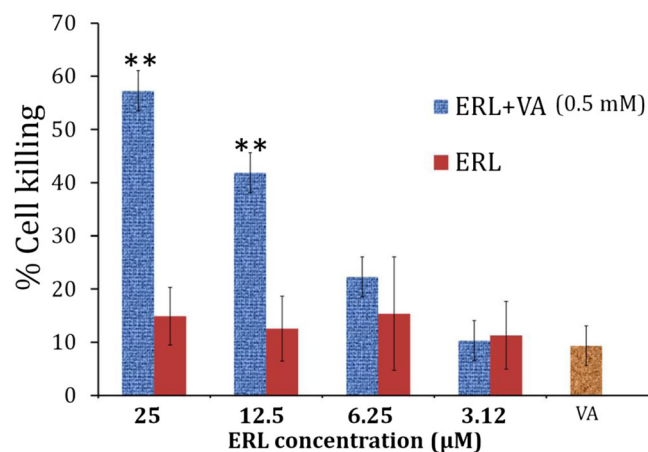


**Fig. 8.** *In vitro* cytotoxicity study of ERL alone and in combination with VA in HCC827/ERL cells. Combination group showed higher cytotoxicity compare to ERL alone group



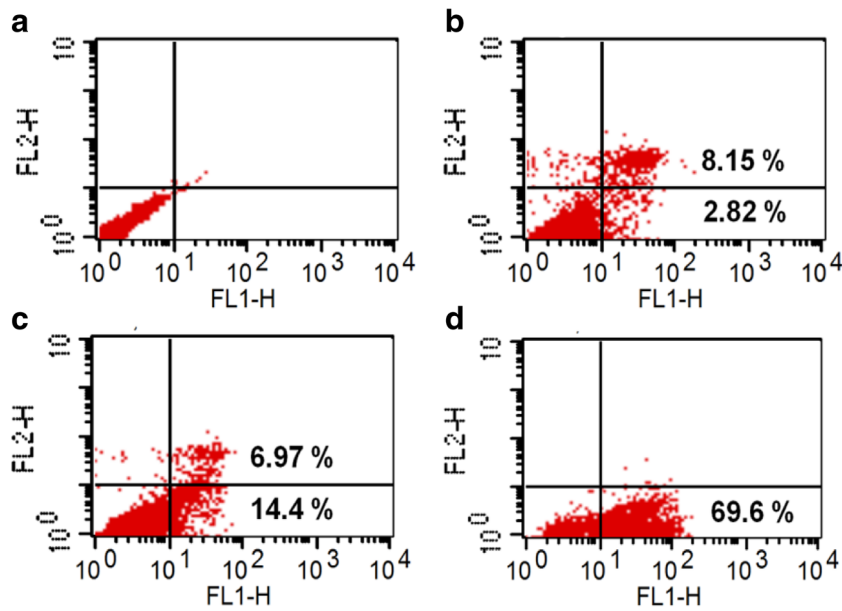


**Fig. 9.** Flow cytometry analysis of **a** control **b** VA **c** ERL **d** ERL + VA-treated HCC827/ERL cells. In the scatter plot of double variable flow cytometry, Q3 quadrant (FITC - / PI-) shows living cells; Q2 quadrant (FITC+/PI+) stands for late apoptotic cells; and Q4 quadrant (FITC+/PI-) represents early apoptotic cells

aluminometasilicate while Aerosil 200 and Aerosil 972 are hydrophilic and hydrophobic colloidal silicon dioxide, respectively. According to data provided by manufacturer—Tomita pharmaceuticals—Florite® has much higher liquid absorption efficiency compared to colloidal silicon dioxide and magnesium aluminosilicates. Results of our studies are very much in agreement with Gumaste *et al.* 2013. We observed that the liquid adsorb deep into the pores of relatively large particles of such adsorbents and release quickly on exposure to aqueous phase (24). Comparison of dissolution profiles in FaSSIF and FeSSIF

indicated that bile components play an important role in the solubilization of ERL. Poor dissolution of ERL in FaSSIF can be explained by its poor solubility at intestinal pH due to weakly basic nature of ERL. FaSSIF has very low concentration of bile salt and lecithin to substantial affect the aqueous solubility of ERL. The increase in the dissolution rate of ERL in FeSSIF can also be explained by the lower pH value of this medium compared to the FaSSIF (5.0 vs. 6.5) and high amount of bile salt and lecithin. In many cases, rapid dissolution of a hydrophobic drug is followed by a precipitation in dissolution medium (25,26).

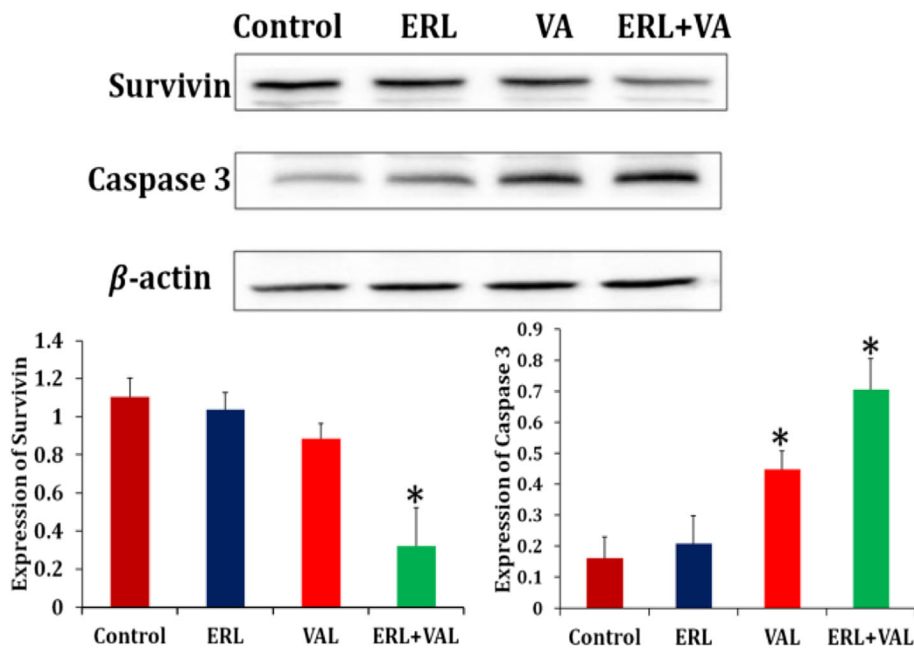


**Fig. 10.** Western blot analysis of apoptosis markers control, VA, ERL, and ERL + VA-treated HCC827/ERL cells

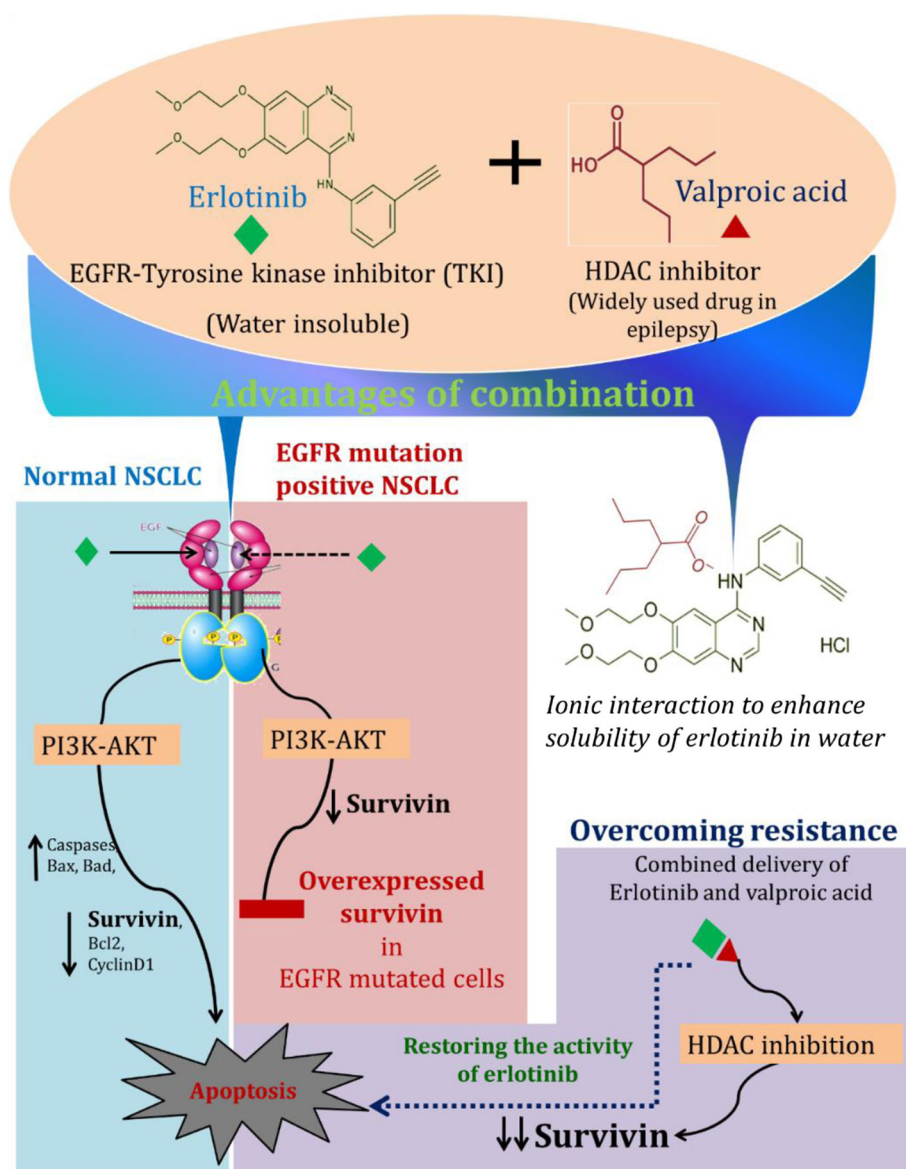


**Fig. 11.** Schematic representation of role of VA in overcoming ERL resistance and enhancing aqueous solubility of ERL

Supersaturated system achieved by rapid dissolution of drug in intestine provides a driving force for nucleation and crystallization. Extensive precipitation in the upper GI tract may result in incomplete absorption and suboptimal systemic exposure (27). In such cases, an excipient/technology to prevent precipitation of drug could potentially help in maintaining drug in supersaturated state in the GI tract. Commonly, it is described as a “spring-and-parachute” approach—Initial rapid dissolution and supersaturation “spring” followed by a precipitation inhibiting/retarding effect “parachute” (26,27). Dissolution studies of EVLF in HCl and biorelevant medium (FeSSIF and FaSSIF) suggested that VA and PEG 400 not only promoted the rapid dissolution of ERL but also prevented precipitation in dissolution medium.

The ERL suspension showed the lowest average ERL plasma concentration due to its low solubility and dissolution rate compared to EVLF. In human, ERL is about 60% absorbed after oral administration and the peak plasma levels occur 4 h after dosing (28). There was no significant difference in volume of

distribution of the prepared EVLF formulation and ERL suspension. EVLF formulation showed significantly enhanced oral absorption in comparison with the reference, ERL suspension formulation with relative bioavailability of 199.90%. The EVLF formulation augmented the oral bioavailability of ERL. The higher bioavailability of EVLF preparations could be attributed to improved dissolution profile of ERL in the intestinal milieu and possibility of intestinal lymphatic drug transport.

## CONCLUSION

Valproic acid markedly increased the sensitivity of TKI-resistant lung adenocarcinoma cells to erlotinib by reducing the survivin. Valproic acid also played a key role in improving the dissolution and oral bioavailability of ERL. Thus, liquid formulation of ERL and VA might offer a promising therapeutic approach to the treatment of lung cancer. Most importantly, since majority of anticancer drugs

are poor water-soluble weak base, combined formulation with VA can be helpful in enhancing solubility, oral bioavailability, and possibly enhanced efficacy due to simultaneous inhibition of HDAC.

## ACKNOWLEDGMENTS

The authors would like to thank BASF and Tomita Pharmaceutical for kindly supplying the samples of excipients used in this study.

## COMPLIANCE WITH ETHICAL STANDARDS

**Conflict of Interest** The authors declare that they have no competing interests.

**Publisher's Note** Springer Nature remains neutral with regard to jurisdictional claims in published maps and institutional affiliations.

## REFERENCES

- Brückl W, Tufman A, Huber RM. Advanced non-small cell lung cancer (NSCLC) with activating EGFR mutations: first-line treatment with afatinib and other EGFR TKIs. *Expert Rev Anticancer Ther.* 2017;17(2):143–55.
- Chan BA, Hughes BG. Targeted therapy for non-small cell lung cancer: current standards and the promise of the future. *Transl Lung Cancer Res.* 2015;4(1):36.
- Patel K, Doddapaneni R, Chowdhury N, Boakye CH, Behl G, Singh M. Tumor stromal disrupting agent enhances the anticancer efficacy of docetaxel loaded PEGylated liposomes in lung cancer. *Nanomed (Lond).* 2016;11(11):1377–92.
- Sullivan I, Planchard D. Next-generation EGFR tyrosine kinase inhibitors for treating EGFR-mutant lung cancer beyond first line. *Front Med.* 2017;3:76.
- Goss GD, Spaans JN. Epidermal growth factor receptor inhibition in the management of squamous cell carcinoma of the lung. *Oncologist.* 2016;21:205–13.
- Wu S-G, Shih J-Y. Management of acquired resistance to EGFR TKI-targeted therapy in advanced non-small cell lung cancer. *Mol Cancer.* 2018;17(1):38.
- Biran A, Brownstein M, Haklai R, Kloog Y. Downregulation of survivin and aurora A by histone deacetylase and RAS inhibitors: a new drug combination for cancer therapy. *Int J Cancer.* 2011;128(3):691–701.
- Okamoto K, Okamoto I, Hatashita E, Kuwata K, Yamaguchi H, Kita A, *et al.* Overcoming erlotinib resistance in EGFR mutation-positive non-small cell lung cancer cells by targeting survivin. *Mol Cancer Ther.* 2011.
- Edwards R, Andan C, Lalla R, Lacouture M, O'Brien D, Sequist L. Afatinib therapy: practical management of adverse events with an oral agent for non-small cell lung cancer treatment. *Clin J Oncol Nurs.* 2018;22(5):542–8.
- Ruess DA, Probst M, Marjanovic G, Wittel UA, Hopt UT, Keck T, *et al.* HDACi valproic acid (VPA) and suberoylanilide hydroxamic acid (SAHA) delay but fail to protect against warm hepatic ischemia-reperfusion injury. *PLoS One.* 2016;11(8):e0161233.
- Zhang L, Wang G, Wang L, Song C, Leng Y, Wang X, *et al.* VPA inhibits breast cancer cell migration by specifically targeting HDAC2 and down-regulating survivin. *Mol Cell Biochem.* 2012;361(1–2):39–45.
- Dora CP, Trotta F, Kushwah V, Devasari N, Singh C, Suresh S, *et al.* Potential of erlotinib cyclodextrin nanosponge complex to enhance solubility, dissolution rate, in vitro cytotoxicity and oral bioavailability. *Carbohydr Polym.* 2016;137:339–49.
- Yang KM, Shin IC, Park JW, Kim K-S, Kim DK, Park K, *et al.* Nanoparticulation improves bioavailability of Erlotinib. *Drug Dev Ind Pharm.* 2017;43(9):1557–65.
- Elkadi S, Elsamaligy S, Al-Suwayeh S, Mahmoud H. The development of self-nanoemulsifying liquisolid tablets to improve the dissolution of simvastatin. *AAPS PharmSciTech.* 2017;18(7):2586–97.
- Shokri J, Adibkia K, Javadzadeh Y. Liquisolid technology: what it can do for NSAIDs delivery? *Colloids Surf B: Biointerfaces.* 2015;136:185–91.
- Cheriyian VT, Alsaab H, Sekhar S, Venkatesh J, Mondal A, Vhora I, *et al.* A CARP-1 functional mimetic compound is synergistic with BRAF-targeting in non-small cell lung cancers. *Oncotarget.* 2018;9(51):29680.
- Perrier J, Zhou Z, Dunn C, Khadra I, Wilson CG, Halbert G. Statistical investigation of the full concentration range of fasted and fed simulated intestinal fluid on the equilibrium solubility of oral drugs. *Eur J Pharm Sci.* 2018;111:247–56.
- Kutlehria S, Behl G, Patel K, Doddapaneni R, Vhora I, Chowdhury N, *et al.* Cholecalciferol-PEG conjugate based nanomicelles of doxorubicin for treatment of triple-negative breast cancer. *AAPS PharmSciTech.* 2018;19(2):792–802.
- Patel K, Chowdhury N, Doddapaneni R, Boakye CHA, Godugu C, Singh M. Piperlongumine for enhancing oral bioavailability and cytotoxicity of docetaxel in triple-negative breast cancer. *J Pharm Sci.* 2015;104(12):4417–26.
- Boakye CHA, Patel K, Doddapaneni R, Bagde A, Marepally S, Singh M. Novel amphiphilic lipid augments the co-delivery of erlotinib and IL36 siRNA into the skin for psoriasis treatment. *J Control Release.* 2017;246:120–32.
- Truong DH, Tran TH, Ramasamy T, Choi JY, Lee HH, Moon C, *et al.* Development of solid self-emulsifying formulation for improving the oral bioavailability of erlotinib. *AAPS PharmSciTech.* 2016;17(2):466–73.
- Patel K, Sarma V, Vavia P. Design and evaluation of Lumefantrine—oleic acid self nanoemulsifying ionic complex for enhanced dissolution. *Daru.* 2013;21(1):27.
- Brus J, Albrecht W, Lehmann F, Geier J, Czernek J, Urbanova M, *et al.* Exploring the molecular-level architecture of the active compounds in liquisolid drug delivery systems based on mesoporous silica particles: old tricks for new challenges. *Mol Pharm.* 2017;14(6):2070–8.
- Gumaste SG, Pawlak SA, Dalrymple DM, Nider CJ, Trombetta LD, Serajuddin AT. Development of solid SEDDS, IV: effect of adsorbed lipid and surfactant on tableting properties and surface structures of different silicates. *Pharm Res.* 2013;30(12):3170–85.
- Brouwers J, Brewster ME, Augustijns P. Supersaturating drug delivery systems: the answer to solubility-limited oral bioavailability? *J Pharm Sci.* 2009;98(8):2549–72.
- Liu C, Chen Z, Chen Y, Lu J, Li Y, Wang S, *et al.* Improving oral bioavailability of Sorafenib by optimizing the “spring” and “parachute” based on molecular interaction mechanisms. *Mol Pharm.* 2016;13(2):599–608.
- Sun DD, Lee PI. Haste makes waste: the interplay between dissolution and precipitation of supersaturating formulations. *AAPS J.* 2015;17(6):1317–26.
- Frohna P, Lu J, Eppler S, Hamilton M, Wolf J, Rakhit A, *et al.* Evaluation of the absolute oral bioavailability and bioequivalence of erlotinib, an inhibitor of the epidermal growth factor receptor tyrosine kinase, in a randomized, crossover study in healthy subjects. *J Clin Pharmacol.* 2006;46(3):282–90.